DWT and SWT based Image Super Resolution without Degrading Clarity

KOPPISETTI JHANSI RANI
M.Tech Scholar, Department of Electronics and Communications Engineering, Chaitanya Institute of Science & Technology, India.

S.SRIVIDYA
Assistant Professor, Electronics & Communications Engineering, Chaitanya Institute of Science & Technology, India.

Abstract: **This project presents a self-similarity-based approach that is able to use large groups of similar patches extracted from the input image to solve the SISR problem. It introduce a novel prior leading to the collaborative filtering of patch groups in a 1D similarity domain and couple it with an iterative back-projection framework. The performance of the proposed algorithm is evaluated on a number of SISR benchmark data sets. Without using any external data, the proposed approach outperforms the current non-convolutional neural network-based methods on the tested data sets for various scaling factors. As an extension of this project, Discrete and Stationary Wavelet Decomposition is proposed to improve accuracy levels.**

Key terms: **Single Image Super Resolution (SISR) Neural Network Methods Discrete And Stationary Wavelet Decomposition**

I. Introduction

Super-resolution imaging (SR) is a class of techniques that enhance (increase) the resolution of an imaging system. In optical SR the diffraction limit of systems is transcended, while in geometrical SR the resolution of digital imaging sensors is enhanced.

Super-resolution (SR) is a technique that allows increasing the resolution of a given image. Having applications in many areas, from medical imaging to consumer electronics, several SR methods have been proposed. Currently, the best performing methods are based on Convolutional Neural Networks (CNNs) and require extensive datasets for training. However, at test time, they fail to impose consistency between the super-resolved image and the given low-resolution image, a property that classic reconstruction-based algorithms naturally enforce in spite of having poorer performance. Motivated by this observation, we propose a new framework that joins both approaches and produces images with superior quality than any of the prior methods. Despite the breakthroughs in accuracy and speed of single image super-resolution using faster and deeper convolutional neural networks, one central problem remains largely unsolved: how do we recover the finer texture details when we super-resolve at large upscaling factors? The behavior of optimization-based super-resolution methods is principally driven by the choice of the objective function.

Optical or diffractive super-resolution

Substituting spatial-frequency bands:

Though the bandwidth allowable by diffraction is fixed, it can be positioned anywhere in the spatial-frequency spectrum.

Multiplexing spatial-frequency bands:

An image is formed using the normal pass band of the optical device. Then some known light structure, for example a set of light fringes that is also within the pass band, is superimposed on the target.[8] The image now contains components resulting from the combination of the target and the superimposed light structure, e.g. moiré fringes, and carries information about target detail which simple, unstructured illumination does not. The "super resolved" components, however, need disentangling to be revealed.

Multiple parameter use within traditional diffraction limit

If a target has no special polarization or wavelength properties, two polarization states or non-overlapping wavelength regions can be used to encode target details, one in a spatial-frequency band inside the cut-off limit the other beyond it. Both would utilize normal pass band transmission but are then separately decoded to reconstitute target structure with extended resolution.

Probing near - field electromagnetic disturbance

The usual discussion of super-resolution involved conventional imagery of an object by an optical system. But modern technology allows probing the electromagnetic disturbance within molecular distances of the source [6] which has superior resolution properties, see also evanescent waves and the development of the new Super lens.

Geometrical or image-processing super-resolution

Multi-exposure image noise reduction

When an image is degraded by noise, there can be more detail in the average of many exposures, even within the diffraction limit. See example on the right.

Single-frame deblurring

Known defects in a given imaging situation, such as defocus or aberrations, can sometimes be mitigated in whole or in part by suitable spatial-frequency filtering of even a single image. Such procedures all stay within the diffraction-mandated pass band, and do not extend it.

Sub - pixel image localization: The location of a single source can be determined by computing the "center of gravity" (centroid) of the light distribution extending over several adjacent pixels (see figure on the left). Provided that there is enough light, this can be achieved with arbitrary precision, very much better than pixel width of the detecting apparatus and the resolution limit for the decision of whether the source is single or double. This technique, which requires the presupposition that all the light comes from a single source, is at the basis of what has become known as super-resolution microscopy, e.g. stochastic optical reconstruction microscopy (STORM), where fluorescent probes attached to molecules give nanoscale distance information. It is also the mechanism underlying visual hyperacuity. [10]

Bayesian induction beyond traditional diffraction limit

Some object features, though beyond the diffraction limit, may be known to be associated with other object features that are within the limits and hence contained in the image. Then conclusions can be drawn, using statistical methods, from the available image data about the presence of the full object.[11] The classical example is Toraldo di Francia's proposition[12] of judging whether an image is that of a single or double star by determining whether its width exceeds the spread from a single star. This can be achieved at separations well below the classical resolution bounds, and requires the prior limitation to the choice "single or double?"

The approach can take the form of extrapolating the image in the frequency domain, by assuming that the object is an analytic function, and that we can exactly know the function values in some interval. This method is severely limited by the ever-present noise in digital imaging systems, but it can work for radar, astronomy, microscopy or magnetic resonance imaging.[13] More recently, a fast single image super-resolution algorithm based on a closed-form solution to problems has been proposed and demonstrated to accelerate most of the existing Bayesian super-resolution methods significantly.

In recent years, these shortcomings have been partially resolved by approaches that use machine learning to generate a low resolution (LR) to high resolution (HR) mapping from a large number of images [29], [38]. Existing methods utilized to learn this mapping include manifold learning [4], sparse coding [42], convolutional neural networks (CNNs) [11], [24], [25], and local linear regression [37], [38]. The prior learned by these approaches has been shown to effectively capture natural image structure, however, the improved performance comes with some strong limitations. First, they heavily rely on a large amount of training data, which can be very specific for different kind of images and somehow limits the domain of application. Second, a number of these approaches, most markedly the CNN based one's, take a considerable amount of training time, ranging from several hours to several days on very sophisticated graphical processing units (GPUs). Third, a separate LR-HR mapping must be learned for each individual up-sampling factor and scale ratio, limiting its use to applications was known beforehand. Finally, a number of these approaches [37], [38], do not support non-integer up-sampling factors.

Certain researchers have addressed the SISR problem by exploiting the priors from the input image in various forms of self-similarity [20], [18], [6], [13]. Freedman and Fattal [18] observed that, although fewer in number, the input image based search results in "more relevant patches". Some self- similarity based algorithms find a LR-HR pair by searching for the most similar target patch in the down-sampled image [18], [20], [23], [32]. Other approaches are able to use several self-similar patches and couple them with sparsity based approaches, such as Dong *et al.* [13]. Yang and Wang [44] are also able to self-learn a model for the reconstruction using sparse representation of image patches. Shi and Qi [30] use a low-rank representation of non-local self-similar patches extracted from different scales of the input image. These approaches do not required training or any external data, but their performance is usually inferior to approaches employing external data, especially on natural images with complex structures and low degree of self-similarity. Still, in all of them, sparsity is regarded as an instrumental tool in improving the reconstruction performance over previous attempts.

In this work we propose Wiener filter in Similarity Domain for Super Resolution (WSD-SR), a technique for SISR that simultaneously considers sparsity and consistency. To achieve this aim, we formulate the SISR problem as a minimization of reconstruction error subject to a sparse self-similarity prior. The core of this work lies in the design of the regularizer that enforces sparsity in groups of self-similar patches extracted from the input image. This regularizer, which we term Wiener filter in Similarity Domain (WSD), is based on Block Matching 3D (BM3D) [7], [8], but includes particular twists that make a considerable difference in SISR tasks. The most significant one is the use of a 1D Wiener filter that only operates along the dimension of similar patches.

II. Existing Methodology

The previous conference publication of the proposed approach was done in [15]. The algorithm in this paper follows the general structure of [15], but introduces a novel regularizer that proved crucial for obtaining significantly improved performance. The distinctive features of the developed algorithm are:

- 1D Wiener filtering along similarity domain;

- Reuse of grouping information;

- Adaptive search window size; Iterative procedure guided by input dependent heuristics;

- Improved parameter tuning.

An extensive simulation study demonstrates the advanced performance of the developed algorithm as compared with [15] and some state-of-the-art methods in the field.

The SISR algorithms can be broadly divided into two main classes: the methods that rely solely on observed data and those that additionally use external data. Both of these classes can be further divided into the following categories: learning- based and reconstruction-based. However, we are going to present below the related work in a simplified division of the methods that only accounts for use, or lack of use, of external data without any aim to be considered as an extensive review of the field.

A. Approaches Using External Data

This type of approaches use a set of HR images and their down-sampled LR versions to learn dictionaries, regression functions or end-to-end mapping between the two. Initial dictionary-based techniques created a correspondence map between features of LR patches and a single HR patch [19]. Searching in this type of dictionaries was performed using approximate nearest neighbours (ANN), as exhaustive search would be prohibitively expensive. Still, dictionaries quickly grew in size with the amount of used training data. Chang *et al.* [4] proposed the use of locally linear embedding (LLE) to better generalize over the training data and therefore require smaller dictionaries. Image patches were assumed to live in a low dimensional manifold which allowed the estimation of high resolution patches as a linear combination of multiple *nearby* patches. Yang *et al.* [42] also tackled to problem of growing dictionary sizes, but using sparse coding. In this case, a technique to obtain a sparse "compact dictionary" from the training data is proposed. This dictionary is then used to find a sparse activation vector for a given LR patch. The HR estimate is finally obtained by multiplying the activation vector by the HR dictionary. Yang *et al.* [43], Zeyde *et al.* [47] build on this approach and propose methods to learn more

compact dictionaries. Ahmed and Shah [1] learns multiple dictionaries, each containing features along a different direction. The high-resolution patch is reconstructed using the dictionary that yields the lowest sparse reconstruction error. Kim and Kim [26] does away with the expensive search procedure by using a new feature transform that is able to perform simultaneous feature extraction and nearest neighbor identification. Dictionaries can also be leveraged together with regression based techniques to compute projection matrices that, when applied to the LR patches, produce a HR result. The papers by Tim ofte*et al.* [37]–[39] are examples of such an approach where for each dictionary atom, a projection matrix that uses only the nearest atoms is computed. Reconstruction is performed by finding the nearest neighbor of the LR patch and employing the corresponding projection matrix. Zhang *et al.* [48] follows a similar approach but also learns the clustering function, reducing the required amount of anchor points. Other approaches do not build dictionaries out of the training data, but chose to learn simple operators, with the advantage of creating more computationally efficient solutions. Tang and Shao [36] learns two small matrices that are used on image patches as left and right multiplication operator and allow fast recovery of the high resolution image. The global nature of these matrices, however, fails to capture small details and complex textures. Choi and Kim [5] learns instead multiple local linear mappings and a global regressor, which are applied in sequence to enforce both local and global consistency, resulting in better representation of local structure. Sun *et al.* [35] learns a prior and applies it using a conventional image restoration approach. Finally, neural networks have also been explored to solve this problem, in various ways. Sidike *et al.* [31] uses a neural network to learn a regressor that tries to follow edges. Zeng *et al.* [46] proposes the use of coupled deep auto encoder (CDA) to learn both efficient representations for low and high resolution patches as well as a mapping function between them. However, a more common use of this type of computational model is to leverage massive amounts of training data and learn a direct low to high resolution image mapping [12], [24], [25], [27]. Of these approaches, only Liu *et al.* [27] tries to include domain expertise in the design phase, and despite the fact that testing is relatively inexpensive, training can take days even on powerful computers.

Although these approaches learn a strong prior from the large amount of training data, they require a long time to train the models. Furthermore, a separate dictionary is trained for each up-sampling factor, which limits the available up-sampling factors during the test time.

B. Approaches Based Only on Observed Data

This type of approaches rely on image priors to

generate an HR image having only access to the LR observation. Early techniques of this sort are still heavily used due to their computational simplicity, but the low order signal models that they employ fail to generate the missing high frequency components, resulting in over-smoothed estimates.

· An alternative approach to image modeling draws from the concept of self-similarity, the idea that natural images exhibit high degree of repetitive behavior. Ebrahimi and Vrscay [14] proposed a super-resolution algorithm by exploiting the self- similarity and the fractal characteristic of the image at different scales, where the non-local means [3] is used to perform the weighting of patches. Freedman and Fattal [18] extended the idea by imposing a limit on the search space and, thereby, reduced the complexity. They also incorporated incremental up-sampling to obtain the desired image size. Suetake *et al.* [34] utilized the self-similarity to generate an example code-book to estimate the missing high-frequency band and combined it with a framework similar to [19]. Glasner *et al.* [20] used self-examples within and across multiple image scales to regularize the otherwise ill-posed classical super-resolution scheme. Singh *et al.* [33] proposed an approach for super-resolving the image in the noisy scenarios. Egiazarian and Katkovnik [15], introduced the sparse coding in the transform domain to collectively restore the local structure in the high resolution image. Dong *et al.* [13] also employs self-similarity to model each pixel as a linear combination of its non-local neighbors. Cui *et al.* [6] utilized the self- similarity with a cascaded network to incrementally increase the image resolution. Recently, Huang *et al.* [23] improved the search strategy by considering affine transformations, instead of translations, for the best patch match. Further, various search strategies have been proposed to improve the LR-HR pair based on textural pattern [32], optical flow [49] and geometry [17].

III Proposed Approach

The proposed regularizer, WSD, is highly influenced by the BM3D collaborative filtering scheme that explores self- similarity of natural images

```
Algorithm 1 WSD-SR Algorithm
    Input: y: low resolution input
    Input: H: sampling operator
    Input: K: number of iterations
    Output: High resolution estimate
 1: U = (H^T H)^+ H^T {up-sampling matrix}
 2: x^0 = Uy {initial estimate}
 3: for k = 1 to K do
 4:    x̃^k = WSD(x^{k-1}, τ_θ^k)
 5:    x^k = αU(y − Hx̃^k) + x̃^k
 6: end for
 7: return x^K
```

As shown in Fig. 1 and further described in Procedure 2, WSD operates in two sequential stages,

both filtering groups of similar patches, as measured using the Euclidean distance. The result of each stage is created by placing the filtered patches back in their original locations and performing simple average for pixels with more than one estimate. The two stages employ different filters on the patch groups. The first stage, which is producing a pilot estimate used by the second stage, uses HT in the 3D transform domain. The second stage on the other hand, which is generating the final result, uses the result of the first stage to estimate an empirical Wiener filter in the 1D transform domain, operating only along the inter-patch dimension, which we call the similarity domain. This filter is then applied to the original input data.

The use of the 1D Wiener filter in the second stage sets this approach apart from both Egiazarian and Katkovnik [15] and Wang *et al.* [40]. It allowed to not only achieve much sharper results and clearer details, but also reduce the computational cost. Furthermore, the employed grouping procedure includes two particular design elements that further improved the sys- tem's performance and reduced its computational complexity: reuse of block match results and adaptive search window size. Finally, as described in the previous section, WSD is applied iteratively in what we term WSD-SR. This requires the modulation of the filtering strength in such a way that it is successively decreased as the steady-state is approached, in a sort of simulated annealing fashion [21]. We present input dependent heuristics for the selection of both the minimum number of iterations and the filter strength curve.

Overall, the main features of our proposal are:

I. Wiener filter in similarity domain;

II. Stateful operation with grouping information reuse;

III. Adaptive search window size;

IV. Input dependent iterative procedure parameters.

These design decisions, as well as the parameters selection are studied in this section. Empirical evidence is presented for each decision, both in terms of reconstruction quality (PSNR) and computational complexity (speed-up factor). The tests were conducted on *Set5* [2] using a scale factor of 4, and sampling operator *H* set to bicubic interpolation with anti- aliasing filter. In all tables, only the feature under analysis changes between the different columns and the column marked with a * reflects the final design.

I. Wiener Filter in Similarity Domain

The original work on collaborative filtering [8] addresses the problem of image denoising, hence, exploits not only the correlation between similar patches but also between pixels of the same patch. It does so by performing 3D Wiener filtering on groups of similar patches. The spectrum of each group is

computed by a separable 3D transform composed of a 2D spatial transform T_{2D} and a 1D transform T_{1D} along the similarity dimension. However, when
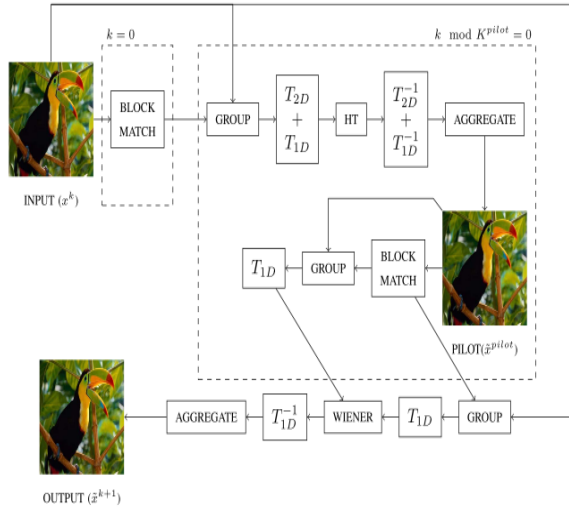

Fig. 1: WSD Block Diagram

dealing with the problem of noiseless super-resolution, employing a 3D Wiener filter results in spatial smoothing, which is further exacerbated by the iterative nature of the algorithm. In order to avoid this problem we use T_{2D} I, which means performing 1D Wiener filtering along the inter-patch similarity dimension. More specifically, given a match table m, a pilot estimate x^{pilot}, and an operation $x(\ , m)$ that extracts from x the patches addressed by m as columns, a 1D empirical Wiener filter W of strength τ_{theta} is estimated as follows:

$$g^{pilot} = \tilde{x}^{pilot}(:, m)$$
$$G^{pilot} = g^{pilot} T_{1D}$$
$$W = \frac{|G^{pilot}|^2}{(|G^{pilot}|^2 + \tau_{theta}^2)}$$

The filter is applied by performing point-wise multiplication with the spectrum of the group of similar patches extracted from the input image x, using the same match table m that was used to estimate the Wiener coefficients W:

$$g^{wiener} = x(:, m)$$
$$G^{wiener} = g^{wiener} T_{1D}$$
$$\tilde{G}^{wiener} = W .* G^{wiener}$$
$$\tilde{g}^{wiener} = T_{1D}^{-1} \tilde{G}^{wiener}$$

The resulting filtered group of patches g^{wiener} is

ready to be aggregated.

These operations are presented in Procedure 2 using sym- bolic names. There, the Group() operation stands for $x(\ , m)$, EstimateWiener() stands for equations (23)-(24) and Wiener- Filter() stands for equations (26)-(28).

Algorithm 2 WSD Algorithm

Input: x: filter input
Input: τ_θ: filter strength
Input: K^{pilot}: pilot recompute period
Input: k: current iteration
Output: $\tilde{x}$: estimate
    {Compute match table for pilot estimation.}
1: **if** $k = 0$ **then**
2:    $m^{ht} \leftarrow$ HTBlockMatch (x)
3: **else**
4:    $m^{ht} \leftarrow m^{ht}_{previous}$
5: **end if**
6:
7: {Pilot estimation.}
8: **if** $k \bmod K^{pilot} = 0$ **then**
9:    $g^{ht} \leftarrow$ Group (x, m^{ht})
10:   $\tilde{g}^{ht} \leftarrow$ HardThresholding (g^{ht}, τ_θ)
11:   $\tilde{x}^{pilot} \leftarrow$ Aggregate $(\tilde{g}^{ht})$
12:   $m^{pilot} \leftarrow$ WienerBlockMatch $(\tilde{x}^{pilot})$
13: **else**
14:   $\tilde{x}^{pilot} \leftarrow \tilde{x}^{pilot}_{previous}$
15:   $m^{pilot} \leftarrow m^{pilot}_{previous}$
16: **end if**
17:
18: {Filter the input image using pilot information.}
19: $g^{pilot} \leftarrow$ Group $(\tilde{x}^{pilot}, m^{pilot})$
20: $W \leftarrow$ EstimateWiener (g^{pilot}, τ_θ)
21: $g^{wiener} \leftarrow$ Group (x, m^{pilot})
22: $\tilde{g}^{wiener} \leftarrow$ WienerFilter (g^{wiener}, W)
23: $\tilde{x} \leftarrow$ Aggregate $(\tilde{g}^{wiener})$
24:
25: {Store information for future reuse.}
26: $m^{ht}_{previous} \leftarrow m^{ht}$
27: $\tilde{x}^{pilot}_{previous} \leftarrow \tilde{x}^{pilot}$
28: $m^{pilot}_{previous} \leftarrow m^{pilot}$
29:
30: **return** $\tilde{x}$

Besides dramatically improving the reconstruction quality, this feature significantly reduces the computational complexity of WSD when compared to a 3D transform based approach, as suggested by the empirical evidence in Table I.

II. Grouping Information Reuse

In the proposed approach, we apply collaborative filtering iteratively on the input image. However, because the structure of the image does not change significantly between iterations, the set of similar patches remains fairly constant. Therefore, we

decided to perform block matching sparsely and reuse the match tables. We observed that in doing so, we not only gain in terms of reduced computational complexity, but also in terms of reconstruction quality. We speculate that the improved performance stems from the fact that by using a set of similar patches for several iterations we avoid oscillations between local minima, and by revising it sporadically, we allow for small structural changes that reflect the contribution of the estimated high frequencies.

Each iteration of the collaborative filter typically requires the execution of the grouping procedure twice, the first time to generate the grouping for HT and the second one to generate the grouping for Wiener filtering. We observed that this iterative procedure is fairly robust to small changes on the grouping used for the HT stage, to the point that optimal results are achieved when that match table is computed only once. The same is not true for the Wiener stage's match table, which still needs to be computed every few iterations,

K^{pilot} in Procedure 2. Table II presents the empirical evidence concerning these observations.

TABLE II

Match Table Reuse Effect On Performance (*Set5*, X4). K^{Pilot}=5. Speedup Is A Factor Relative To Match Table Reuse: Disabled

Match table reuse	Disabled	Enabled*	
	PSNR	PSNR	Speedup
Baby	33.50	33.55	2.82
Bird	33.12	33.25	3.01
Butterfly	27.25	27.45	3.23
Head	32.66	32.65	2.92
Woman	29.98	30.04	3.14
Average	31.30	31.39	3.02

III. *Adaptive Search Window Size*

A straightforward solution to define the search window size for block matching would be to use the whole image as the search space. In doing so, we would be in the situation of global self-similarity and guarantee the selection of all the available patches meeting the similarity constraint. There are, however, two drawbacks to this solution. First, it incurs a significant computational overhead as the complexity grows quadratically with the radius of the search window. Second, it inevitably results in the inclusion of certain patches that, although close to the reference patch in the Euclidean space, represent very different structures in the image.

This effect can be observed in Fig. 2a, specifically

on the top patch, where global self-similarity results in the selection of patches which do not lie on the butterfly and have very differ- ent surrounding structure compared to the reference patch. An alternative solution would be limit the search window to a small neighborhood of the reference patch. However, if the search window is too small, it might happen that not enough similar patches can be found, as exemplified in Fig. 2b. In our proposal we use an incremental approach that starts with a small search window and enlarges it just enough to find a full group of patches which exhibit an Euclidean distance to the reference patch smaller that a preset value. Fig. 2c
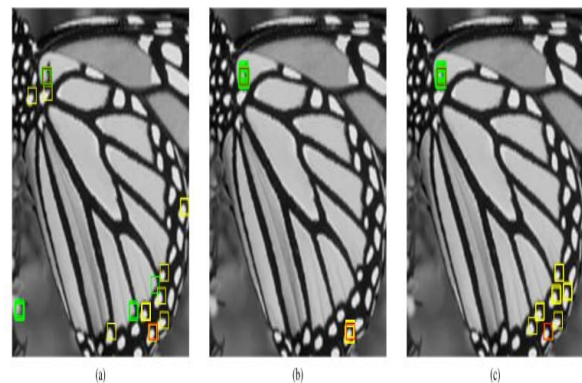

Fig. 2. Three types of search strategies. Global, local and incremental. Red blocks indicate the reference patches. Green patches denote the matching patches for the reference patch at the top of the butterfly. Yellow patches denote the matching results corresponding to the reference at the bottom of the butterfly. (a) Global. (b) Local. (c) Incremental.

shows an example where this incremental strategy finds similar patches from the local region for both reference blocks.

We tested the three different definitions of the search space here discussed, aiming to find 32 similar patches, resulting in Table III. It can be observed that for some images, the use of global search results in a drop of performance, while the use of incremental search never compromises the reconstruction quality.

IV. *Iterative Procedure Parameters*

The iterative nature of the proposed solution introduces the need to select two global parameters that significantly affect the overall system performance: the total number of iterations and the collaborative filter strength curve, τ_θ.

We use an inverse square filter strength curve, with fixed starting and end point, as described in the following equation:

$$\tau_\theta^k = \gamma_k \frac{(K-k)^2}{K} + \gamma_s s$$

Here *K* is the total number of iterations, *k* is the current iteration and *s* is the scale factor. This curve will lead to slower convergence when more iterations are used and vice-versa, allowing the number of iterations to be adjusted freely.

In order to devise a rule for the selection of the number of iterations, we studied the convergence of the method by reconstruction various images of *Set5* using a different number of iterations.

IV Results

A. Quantitative Analysis: It can be observed that the proposed approach outperforms all but the more recent CNN based methods: VDSR and DRCN. Note that these two methods used external data and reportedly require 4 hours and 6 days to generate the necessary models, contrary to our approach that relies solely on the image data. Comparing to the only other self-similarity based method, SelfEx [23], the proposed method shows considerable better performance, implying that the collaborative processing of the mutually similar patches provides a much stronger prior than the single most similar patch from the input image. We also note that for high up-sampling factors of *Urban100*, the performance of the proposed method is in par with even the CNN based methods, showing that this approach is especially suited for images with a high number of edges and marked self-similarity. It also confirms that hypothesis that the self-similarity based priors, although less in number, are very powerful, and can compete with dictionaries learned over millions of patches. Finally we note that the use of Wiener filter in similarity domain shows a significant performance improvement over the use of Wiener filter in 3D transform domain, which further supports our hypothesis that this specific feature is indeed crucial for the overall performance of the proposed approach.

B. Qualitative Analysis: So far we evaluated the proposed approach on a benchmark used for SISR performance assessment. Here we extend our analysis by providing a discussion on the visual quality of the results obtained by various methods. The analysis is conducted on results obtained with up-scaling factor of 4.

C. Comparison With Varying Number of Iterations

We investigate the effect of having a fixed number of iterations on the performance of the proposed approach, when compared with other approaches, as opposed to using the estimation method presented in Section V-D. We can see that with a few dozen iterations our method outperforms most of the other approaches, most notably the self-similarity based SelfEx. With a further increase in number of iterations it is even capable of achieving similar results as the

state of the art convolutional network based approach VDSR.

Next, we plot the computation time against the number of iterations. We also show the computation time of the other approaches in a way that allows easy comparison.
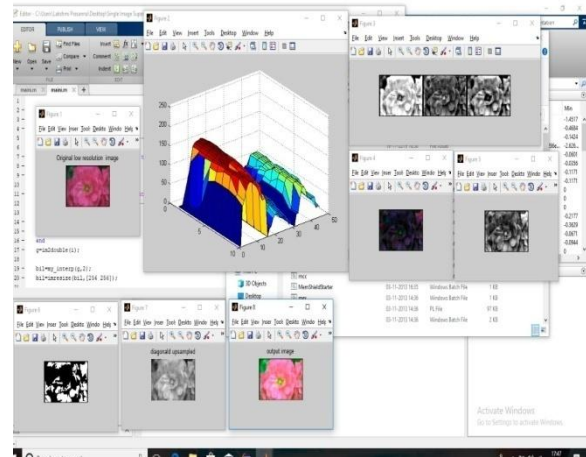

Fig. 3 Single Image Super Resolution

Note however that the number of iterations is only relevant to WSD-SR. All other approaches were executed in their canonical state, using the publicly available codes. As expected, for WSD-SR the computation time increases linearly with the number of iterations. It can be observed that the proposed approach is generally slower than the dictionary based methods. Note also that even at 400 iterations, the proposed approach still performs faster than the only method for which we can't match the reconstruction performance, DRCN. Compared to the self-similarity based approach [23], the proposed algorithm is able to achieve comparable results much faster, and about 1dB better at the break even point. In WSD-SR, the number of iterations can provide a trade- off between the performance and the processing time of the algorithm.

Conclusion

The main progress in SRtechniques can basically be divided into three stages. In the first decade, researchers shifted their attention from the study of frequency domain methods to spatial domain algorithms. Regularized multi frame SR frame work were the main focus in the second stage. This work shown that 1D Wiener filtering along the similarity domain is more effective for the specific problem of SISR and results in much sharper reconstructions. Our novel collaborative filter, WSD, is able to achieve state-of-the-art results when coupled with iterative

back-projection, a combination we termed WSD-SR. combination of DWT and SWT yields an excellent results for super resolution enhancement with atmost optimized parameters.

References

[1] L. Yi-bo, X. Hong, and Z. Sen-yue, "The wrinkle generation method for facial reconstruction based on extraction of partition wrinkle line features and fractal interpolation," in *Proc. 4th Int. Conf. Image Graph.*, Aug. 22–24, 2007, pp. 933–937.

[2] Y. Rener, J. Wei, and C. Ken, "Downsample-based multiple description coding and post-processing of decoding," in *Proc. 27th Chinese Control Conf.*, Jul. 16–18, 2008, pp. 253–256.

[3] H. Demirel, G. Anbarjafari, and S. Izadpanahi, "Improved motionbased localized super resolution technique using discrete wavelet transform for low resolution video enhancement," in *Proc. 17th Eur. Signal Process. Conf.*, Glasgow, Scotland, Aug. 2009, pp. 1097–110 .

[4] Y. Piao, I. Shin, and H. W. Park, "Image resolution enhancement using inter-subband correlation in wavelet domain," in *Proc. Int. Conf. Image Process.*, 2007, vol. 1, pp. I-445–448.

[5] H. Demirel and G. Anbarjafari, "Satellite image resolution enhancement using complex wavelet transform," *IEEE Geoscience and Remote Sensing Letter*, vol. 7, no. 1, pp. 123–126, Jan. 2010.

[6] C. B. Atkins, C. A. Bouman, and J. P. Allebach, "Optimal image scaling using pixel classification," in *Proc. Int. Conf. Image Process.*, Oct. 7–10, 2001, vol. 3, pp. 864–867.

[7] W. K. Carey, D. B. Chuang, and S. S. Hemami, "Regularity-preserving image interpolation," *IEEE Trans. Image Process.*, vol. 8, no. 9, pp. 1295–1297, Sep. 1999.

[8] S. Mallat, *A Wavelet Tour of Signal Processing*, 2nd ed. New York: Academic, 1999.

[9] J. E. Fowler, "The redundant discrete wavelet transform and additive noise,"Mississippi State ERC, Mississippi State University, Tech. Rep MSSU-COE-ERC-04-04, Mar. 2004.

[10] X. Li and M. T. Orchard, "New edge-directed interpolation," *IEEE Trans. Image Process.*, vol. 10, no. 10, pp. 1521–1527, Oct. 2001.

[11] K. Kinebuchi, D. D. Muresan, and R. G. Baraniuk, "Waveletbased statistical signal processing using hidden Markov models," in *Proc. Int. Conf. Acoust., Speech, Signal Process.*, 2001, vol. 3, pp. 7–11.

[12] S. Zhao, H. Han, and S. Peng, "Wavelet domain HMT-based image super resolution," in *Proc. IEEE Int. Conf. Image Process.*, Sep. 2003, vol. 2, pp. 933–936.

[13] A. Temizel and T. Vlachos, "Wavelet domain image resolution enhancement using cycle-spinning," *Electron.Lett.*, vol. 41, no. 3, pp. 119–121, Feb. 3, 2005.

[14] A. Temizel and T. Vlachos, "Image resolution upscaling in the wavelet domain using directional cycle spinning," *J. Electron. Imag.*, vol. 14, no. 4, 2005.

[15] G. Anbarjafari and H. Demirel, "Image super resolution based on interpolation of wavelet domain high frequency subbands and the spatial domain input image," *ETRI J.*, vol. 32, no. 3, pp. 390–394, Jun. 2010.

[16] A. Temizel, "Image resolution enhancement using wavelet domain hidden Markov tree and coefficient sign estimation," in *Proc. Int. Conf. Image Process.*, 2007, vol. 5, pp. V-381–384.